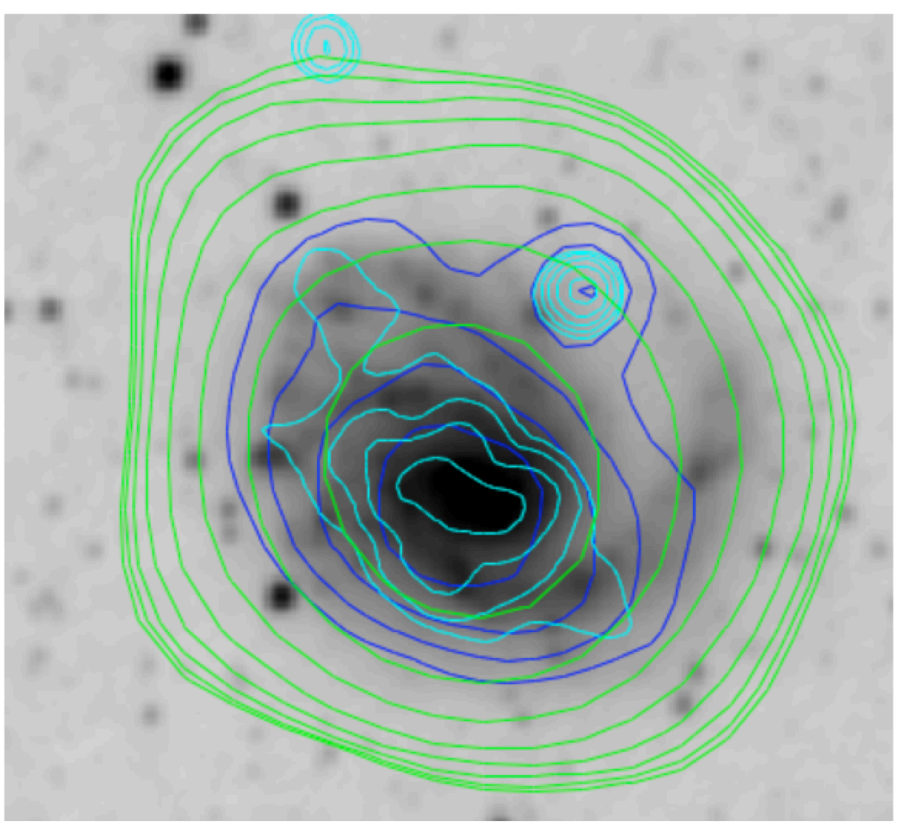

International Centre for Radio Astronomy Research

The Surprising Complexity of the Radio Emission from Star Forming Galaxies

Nick Seymour (ICRAR/Curtin) & Tim Galvin (WSU)

Bologna – #TBILFO2017 - 22nd June 2017

Curtin University

The University of Western Australia

Star Formation History of the Universe

Science Goal	SWG	Objective	SWG Rank
1	*CD/EoR*	Physics of the early universe IGM - I. Imaging	1/3
2	*CD/EoR*	Physics of the early universe IGM - II. Power spectrum	2/3
4	*Pulsars*	Reveal pulsar population and MSPs for gravity tests and Gravitational Wave detection	1/3
5	*Pulsars*	High precision timing for testing gravity and GW detection	1/3
13	*HI*	Resolved HI kinematics and morphology of ~10^10 M_sol mass galaxies out to z~0.8	1/5
14	*HI*	High spatial resolution studies of the ISM in the nearby Universe.	2/5
15	*HI*	Multi-resolution mapping studies of the ISM in our Galaxy	3/5
18	*Transients*	Solve missing baryon problem at z~2 and determine the Dark Energy Equation of State	=1/4
22	*Cradle of Life*	Map dust grain growth in the terrestrial planet forming zones at a distance of 100 pc	1/5
27	*Magnetism*	The resolved all-Sky characterisation of the interstellar and intergalactic magnetic fields	1/5
32	*Cosmology*	Constraints on primordial non-Gaussianity and tests of gravity on super-horizon scales.	1/5
33	*Cosmology*	Angular correlation functions to probe non-Gaussianity and the matter dipole	2/5
37 + 38	*Continuum*	Star formation history of the Universe (SFHU) – I+II. Non-thermal & Thermal processes	1+2/8

Table 2. List of highest priority SKA1 science objectives, grouped by SWG, but otherwise in arbitrary order.

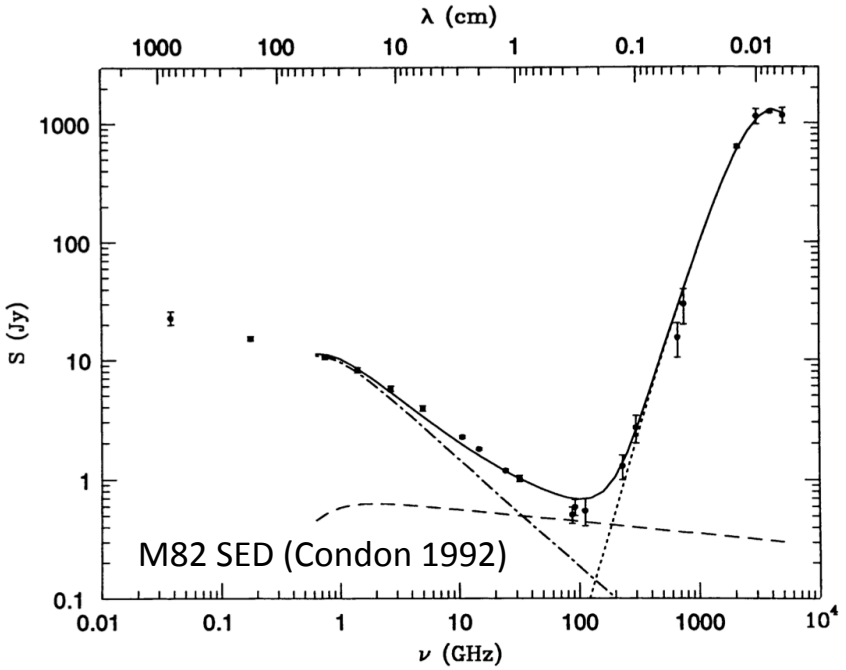

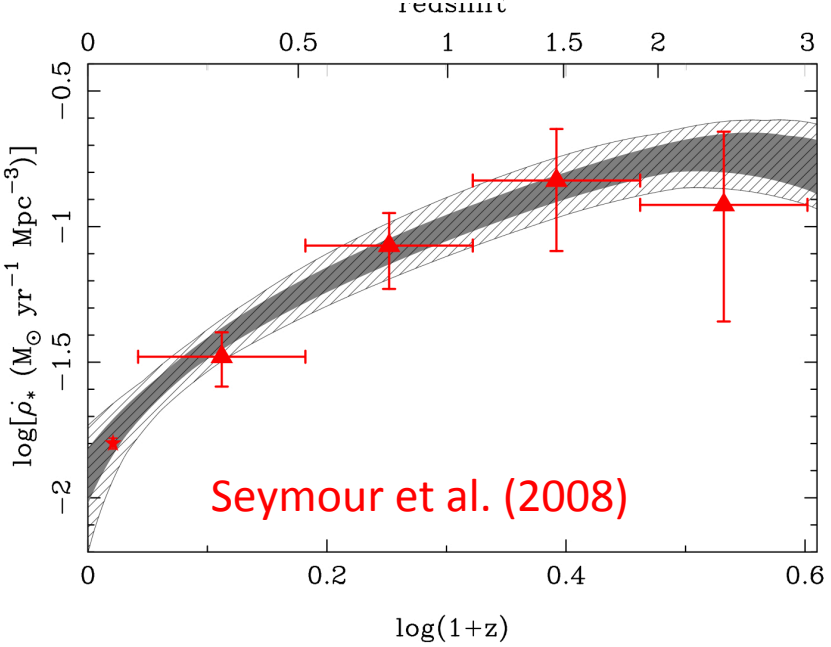

The (Paschen-α) Sample

Work led by Tim Galvin (WSU)

19 sources:

- $S_{60\mu m} > 1.4$ Jy
- $L_{1\text{-}1000\mu m} > 10^{11} L_{\odot}$
- $0.067 < z < 0.227$
- Dec. < -30°
- Remove AGN
  - Optical classification
  - > 5σ away from radio-IR correlation

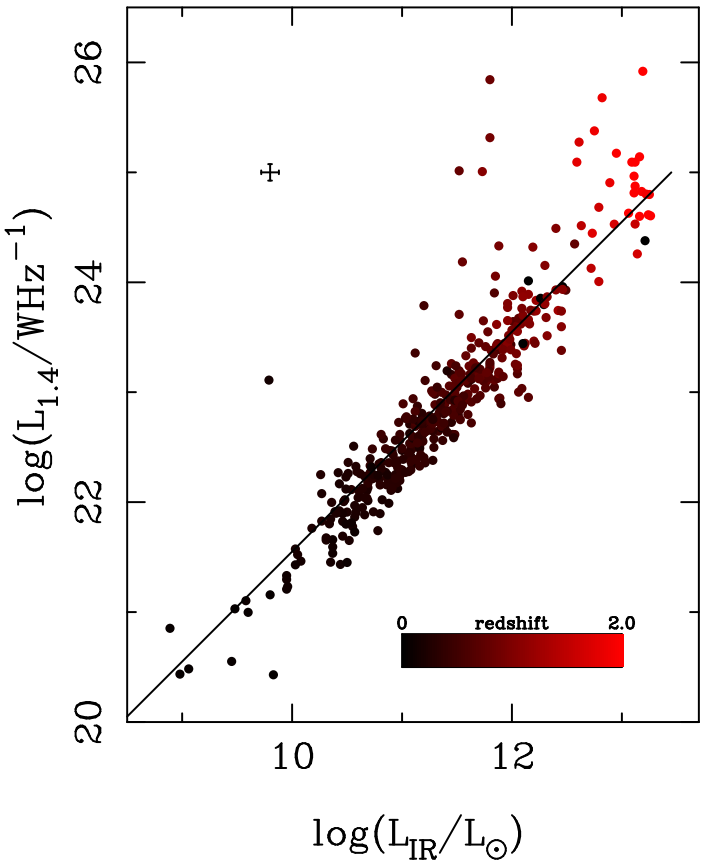

T. Galvin, Seymour, et al. (submitted)

Seymour et al. (2009)

Observations

MWA/GLEAM:

- 70-230 MHz
- All-sky (dec.<+30°)
- 170-230 MHz detection image
- 20 flux measurements
- Priorised flux densities for MWA non-detections at 200MHz

T. Galvin, Seymour, et al. (submitted)

Central Frequency GHz	Band	Array	Date Observed	LAS “
2.1	L/S	6A	23-01-2015	89.0
5.0	C/X	6A	27-01-2015	37.4
5.0	C/X	750C	29-12-2015	275.3
6.8	C/X	6A	27-01-2015	27.5
6.8	C/X	750C	29-12-2015	201.7
8.8	C/X	6A	27-01-2015	21.2
8.8	C/X	750C	29-12-2015	155.9
10.8	C/X	6A	27-01-2015	17.31
10.8	C/X	750C	29-12-2015	127.0
17.0	K	6A	23-01-2015	11.0
17.0	K	750C	31-12-2015	80.9
17.0	K	H168	06-09-2016	60.5
21.0	K	6A	23-01-2015	8.9
21.0	K	750C	31-12-2015	65.3
21.0	K	H168	06-09-2016	49.0
45.0	Q	H214	4-09-2014	17.0
47.0	Q	H214	4-09-2014	15.9
89.0	W	H214	4-09-2014	8.6
93.0	W	H214	4-09-2014	8.2

ATCA Observations: PI T. Galvin

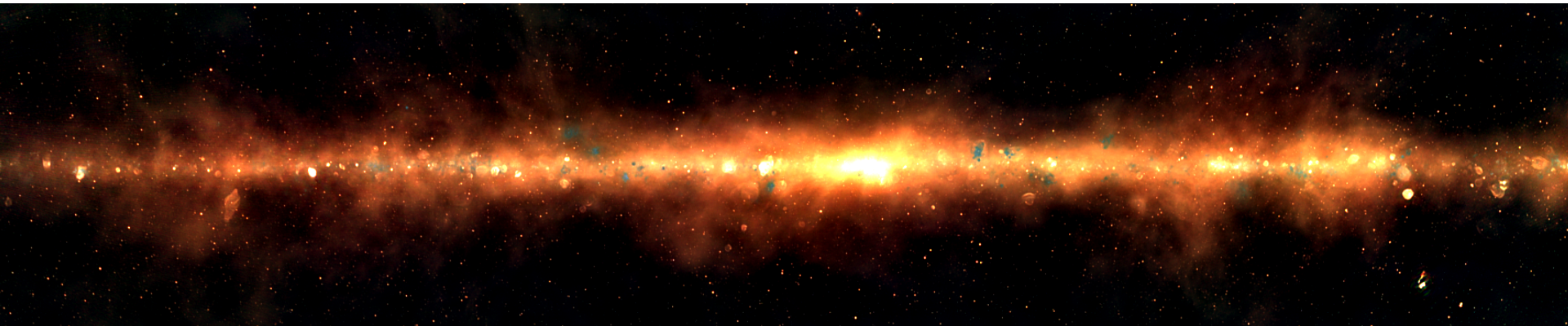

Models

One Component:
Power-law

$$S_\nu = A\left(\frac{\nu}{\nu_0}\right)^{\alpha}. \qquad (1)$$

Power-law + Free-free

$$S_\nu = A\left(\frac{\nu}{\nu_0}\right)^{\alpha} + B\left(\frac{\nu}{\nu_0}\right)^{-0.1}, \qquad (2)$$

Power-law + Free-free + Turn-over

$$S_\nu = (1-e^{-\tau})\left[B + A\left(\frac{\nu}{\nu_{t,1}}\right)^{0.1+\alpha}\right]\left(\frac{\nu}{\nu_{t,1}}\right)^{2}, \qquad (3)$$

Models

One Component:
Power-law

$$S_\nu = A\left(\frac{\nu}{\nu_0}\right)^{\alpha}. \quad (1)$$

Power-law + Free-free

$$S_\nu = A\left(\frac{\nu}{\nu_0}\right)^{\alpha} + B\left(\frac{\nu}{\nu_0}\right)^{-0.1}, \quad (2)$$

Power-law + Free-free + Turn-over

$$S_\nu = (1-e^{-\tau})\left[B + A\left(\frac{\nu}{\nu_{t,1}}\right)^{0.1+\alpha}\right]\left(\frac{\nu}{\nu_{t,1}}\right)^{2}, \quad (3)$$

Two Components:
Same Synchrotron Power-law

$$S_\nu = (1-e^{-\tau_1})\left[B + A\left(\frac{\nu}{\nu_{t,1}}\right)^{0.1+\alpha}\right]\left(\frac{\nu}{\nu_{t,1}}\right)^{2} + (1-e^{-\tau_2})\left[D + C\left(\frac{\nu}{\nu_{t,2}}\right)^{0.1+\alpha}\right]\left(\frac{\nu}{\nu_{t,2}}\right)^{2}, \quad (4)$$

Same Synchrotron Power-law
+ only one turn-over

$$S_\nu = \left(\frac{\nu}{\nu_0}\right)^{-2.1}\left[B + A\left(\frac{\nu}{\nu_0}\right)^{0.1+\alpha}\right]\left(\frac{\nu}{\nu_0}\right)^{2} + (1-e^{-\tau_2})\left[D + C\left(\frac{\nu}{\nu_{t,2}}\right)^{0.1+\alpha}\right]\left(\frac{\nu}{\nu_{t,2}}\right)^{2}. \quad (5)$$

Different Synchrotron Power-law

$$S_\nu = (1-e^{-\tau_1})\left[B + A\left(\frac{\nu}{\nu_{t,1}}\right)^{0.1+\alpha}\right]\left(\frac{\nu}{\nu_{t,1}}\right)^{2} + (1-e^{-\tau_2})\left[D + C\left(\frac{\nu}{\nu_{t,2}}\right)^{0.1+\alpha_2}\right]\left(\frac{\nu}{\nu_{t,2}}\right)^{2}, \quad (6)$$

Models

One Component:
Power-law

$$S_\nu = A\left(\frac{\nu}{\nu_0}\right)^{\alpha}. \quad (1)$$

Power-law + Free-free

$$S_\nu = A\left(\frac{\nu}{\nu_0}\right)^{\alpha} + B\left(\frac{\nu}{\nu_0}\right)^{-0.1}, \quad (2)$$

Power-law + Free-free + Turn-over

$$S_\nu = (1-e^{-\tau})\left[B + A\left(\frac{\nu}{\nu_{t,1}}\right)^{0.1+\alpha}\right]\left(\frac{\nu}{\nu_{t,1}}\right)^{2}, \quad (3)$$

Thermal Infra-red Emission

$$S_\nu(\lambda) = I \times \left[\left(\frac{60\,\mu\mathrm{m}}{\lambda}\right)^{3+\beta} \times \frac{1}{e^{\frac{hc}{\lambda kT}} - 1}\right], \quad (7)$$

Two Components:
Same Synchrotron Power-law

$$S_\nu = (1-e^{-\tau_1})\left[B + A\left(\frac{\nu}{\nu_{t,1}}\right)^{0.1+\alpha}\right]\left(\frac{\nu}{\nu_{t,1}}\right)^{2} + (1-e^{-\tau_2})\left[D + C\left(\frac{\nu}{\nu_{t,2}}\right)^{0.1+\alpha}\right]\left(\frac{\nu}{\nu_{t,2}}\right)^{2}, \quad (4)$$

Same Synchrotron Power-law
+ only one turn-over

$$S_\nu = \left(\frac{\nu}{\nu_0}\right)^{-2.1}\left[B + A\left(\frac{\nu}{\nu_0}\right)^{0.1+\alpha}\right]\left(\frac{\nu}{\nu_0}\right)^{2} + (1-e^{-\tau_2})\left[D + C\left(\frac{\nu}{\nu_{t,2}}\right)^{0.1+\alpha}\right]\left(\frac{\nu}{\nu_{t,2}}\right)^{2}. \quad (5)$$

Different Synchrotron Power-law

$$S_\nu = (1-e^{-\tau_1})\left[B + A\left(\frac{\nu}{\nu_{t,1}}\right)^{0.1+\alpha}\right]\left(\frac{\nu}{\nu_{t,1}}\right)^{2} + (1-e^{-\tau_2})\left[D + C\left(\frac{\nu}{\nu_{t,2}}\right)^{0.1+\alpha_2}\right]\left(\frac{\nu}{\nu_{t,2}}\right)^{2}, \quad (6)$$

Results: Fits

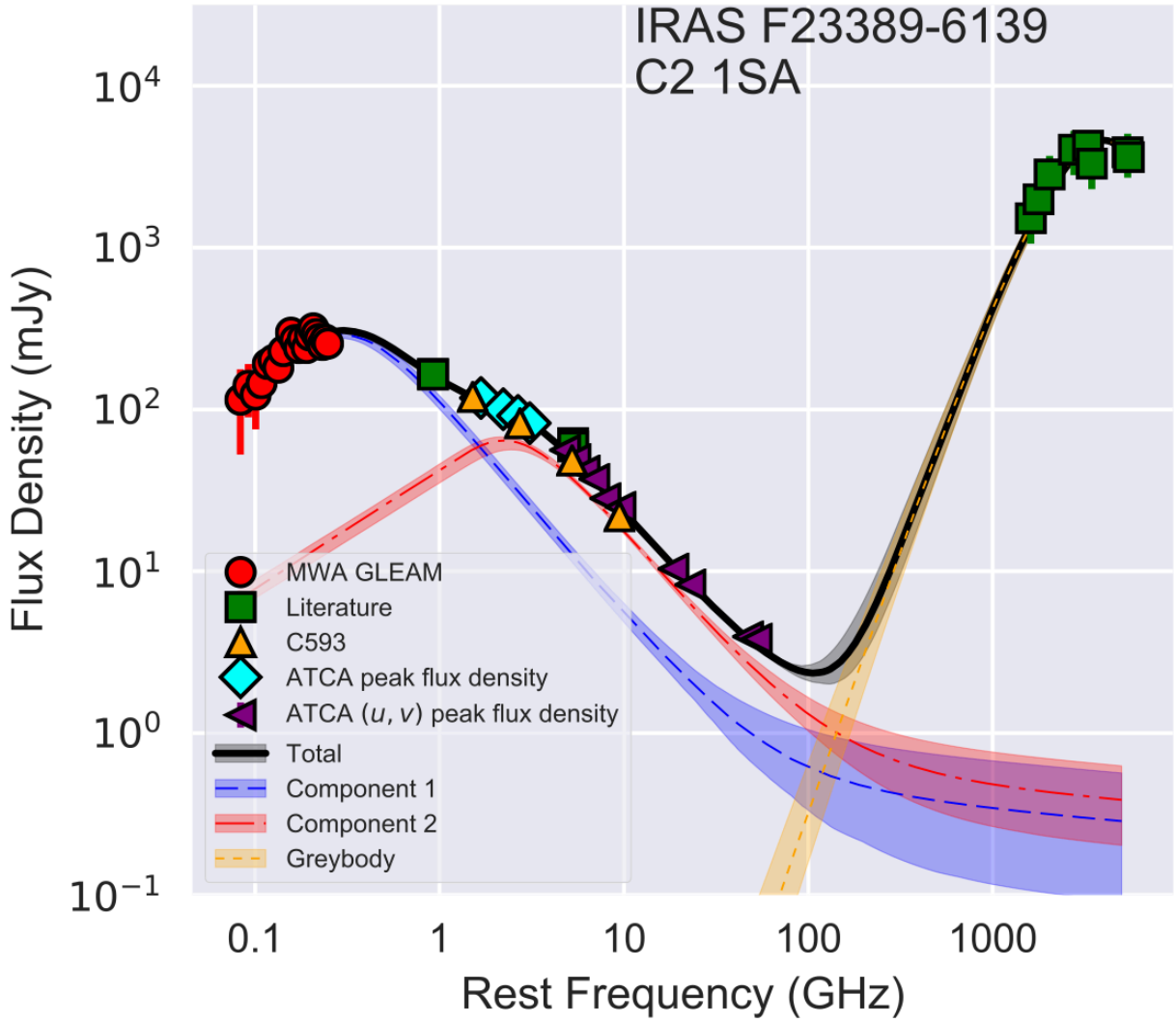

SED complexity only revealed from high fidelity radio observations!

T. Galvin, Seymour, et al. (submitted)

Results: SED Choice

Model	1	2	3	4	5	6
Source *IRAS*	PL	SFG NC	C	C2 1SAN	C2 1SA	C2
F00198-7926	-12.0	-13.2	-15.8	-10.4	***0.0***	*-0.9*
F00199-7426	-15.4	-17.0	*-1.4*	***0.0***	*-1.9*	*-2.2*
F01268-5436	-7.1	***0.0***	*-2.2*	-4.7	-5.1	-5.2
F01388-4618	-12.6	-14.3	***0.0***	*-3.0*	-3.7	-4.5
F01419-6826	***0.0***	*-1.4*	*-0.9*	*-2.3*	*-2.9*	*-2.0*
F02364-4751	-28.5	-30.1	***0.0***	*-2.6*	*-2.4*	*-1.9*
F03068-5346	-9.4	*-0.3*	***0.0***	*-0.9*	*-2.6*	*-1.6*
F03481-4012	***0.0***	*-1.4*	-3.5	-6.5	-3.8	-4.5
F04063-3236	-23.2	-24.8	-30.4	-9.5	***0.0***	*-1.3*
F06021-4509	-8.5	-10.2	-10.4	*-1.8*	*-0.0*	***0.0***
F06035-7102	-53.9	-55.1	-21.7	***0.0***	*-1.7*	-5.4
F06206-6315	-65.8	-67.2	-29.4	-23.1	***0.0***	*-0.3*
F18582-5558	-24.9	-26.5	-22.9	*-0.3*	*-1.1*	***0.0***
F20117-3249	-148.5	-150.0	-18.7	***0.0***	-7.5	-4.3
F20445-6218	*-1.9*	-3.3	***0.0***	*-1.3*	-3.3	*-1.3*
F21178-6349	*-2.5*	-3.2	***0.0***	-4.1	*-1.6*	*-2.1*
F21292-4953	***0.0***	*-1.8*	-4.3	-3.3	-5.9	-5.9
F21295-4634	-20.3	-21.9	*-0.1*	***0.0***	*-2.0*	*-1.0*
F23389-6139	-1451.1	-1452.6	-211.6	-146.5	***0.0***	*-1.1*
Number	3	1	5	4	4	2

Table 4. An overview of the derived evidence values for each of the fitted models obtained using MULTINEST. The evidence value for each source has been normalised to the best supported model. ***Bold-italic*** typeface on blue shaded cells indicates the 'best' model, judged strictly by the evidence value, for each source. *Italic* typeface on green shaded cells highlight competing models whose evidence value is indistinguishable from the 'best' model for each source according to the Bayes odds ratio scale.

Summary:

- 10/19 show multiple components
- 15/19 show low-frequency turn-overs
- 3 are best-fit by a power-law

T. Galvin, Seymour, et al. (submitted)

Power-law Sources

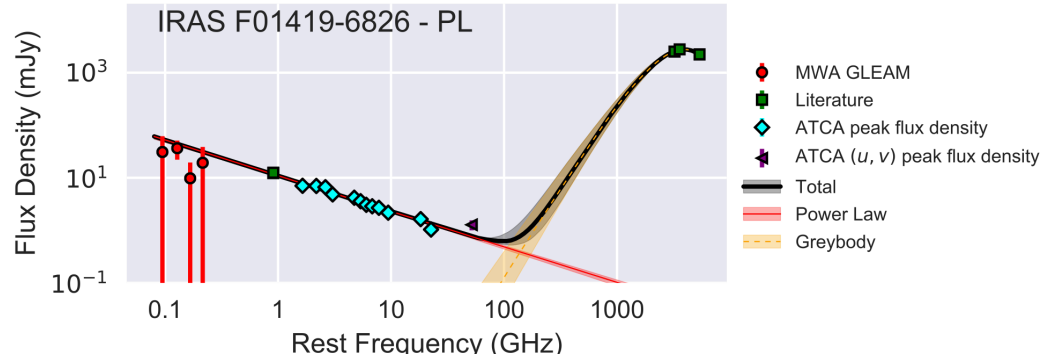

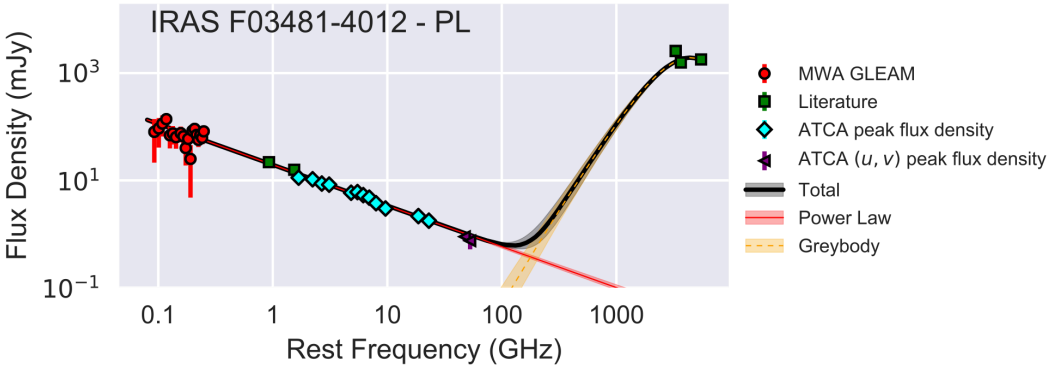

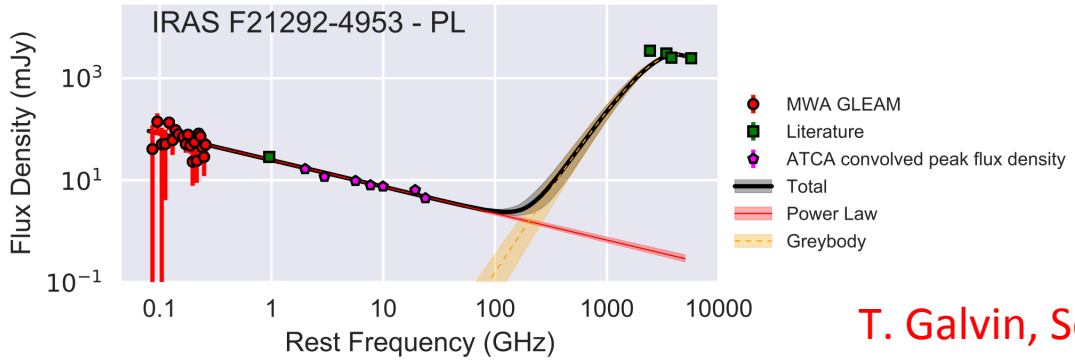

Power-law best-fits may turn-over if we had better S/N

T. Galvin, Seymour, et al. (submitted)

Fit Parameters

Table 5. An overview of the most preferred models judged strictly by their evidence value and their constrained values. We use the 50^{th} percentile of the samples posterior distribution as the nominal value, and use the 16^{th} and 84^{th} percentiles to provide the 1σ uncertainties. Parameters not included in a model are marked by a '–'. We omit parameters constrained that belong to the Matérn covariance function.

Source *IRAS*	Model	A mJy	B mJy	α	$\nu_{t,1}$ GHz	C mJy	D mJy	α_2	$\nu_{t,2}$ GHz	I Jy	Temp. K	β
F00198-7926	C2 1SA	$187.9^{+16.7}_{-15.2}$	$0.5^{+0.6}_{-0.4}$	$-1.3^{+0.1}_{-0.1}$	$0.2^{+0.0}_{-0.0}$	$7.6^{+0.8}_{-1.0}$	$0.5^{+0.4}_{-0.3}$	-	$6.2^{+0.7}_{-0.6}$	$0.23^{+0.06}_{-0.06}$	$55.5^{+4.5}_{-3.2}$	$1.3^{+0.3}_{-0.2}$
F00199-7426	C2 1SAN	$6.4^{+2.6}_{-3.0}$	$0.2^{+0.3}_{-0.2}$	$-0.8^{+0.0}_{-0.0}$	-	$46.6^{+21.8}_{-13.7}$	$0.2^{+0.3}_{-0.2}$	-	$0.5^{+0.2}_{-0.1}$	$1.52^{+0.41}_{-0.29}$	$40.1^{+1.8}_{-1.9}$	$1.1^{+0.2}_{-0.1}$
F01268-5436	SFG NC	$0.8^{+0.2}_{-0.2}$	$12.4^{+0.4}_{-0.4}$	$-1.0^{+0.0}_{-0.0}$	-	-	-	-	-	$0.34^{+0.22}_{-0.12}$	$44.7^{+4.6}_{-4.4}$	$1.3^{+0.4}_{-0.3}$
F01388-4618	C	$44.4^{+5.5}_{-4.2}$	$0.2^{+0.2}_{-0.1}$	$-0.7^{+0.0}_{-0.0}$	$0.3^{+0.0}_{-0.0}$	-	-	-	-	$0.59^{+0.25}_{-0.19}$	$45.7^{+3.8}_{-3.1}$	$1.6^{+0.2}_{-0.3}$
F01419-6826	PL	$8.7^{+0.3}_{-0.3}$	-	$-0.7^{+0.0}_{-0.0}$	-	-	-	-	-	$0.82^{+0.37}_{-0.32}$	$41.2^{+3.7}_{-2.5}$	$1.7^{+0.2}_{-0.4}$
F02364-4751	C	$86.5^{+4.7}_{-4.6}$	$0.3^{+0.3}_{-0.2}$	$-0.8^{+0.0}_{-0.0}$	$0.3^{+0.0}_{-0.0}$	-	-	-	-	$1.04^{+0.43}_{-0.30}$	$40.8^{+2.9}_{-2.4}$	$1.3^{+0.3}_{-0.2}$
F03068-5346	C	$147.1^{+205.1}_{-19.3}$	$2.5^{+0.4}_{-0.5}$	$-0.9^{+0.1}_{-0.1}$	$0.1^{+0.0}_{-0.1}$	-	-	-	-	$0.40^{+0.16}_{-0.08}$	$49.7^{+3.0}_{-3.4}$	$1.2^{+0.2}_{-0.1}$
F03481-4012	PL	$15.0^{+0.3}_{-0.4}$	-	$-0.8^{+0.0}_{-0.0}$	-	-	-	-	-	$0.29^{+0.12}_{-0.09}$	$47.3^{+3.8}_{-3.0}$	$1.5^{+0.3}_{-0.3}$
F04063-3236	C2 1SA	$49.4^{+4.4}_{-4.0}$	$0.2^{+0.3}_{-0.1}$	$-1.3^{+0.1}_{-0.1}$	$0.3^{+0.0}_{-0.0}$	$5.2^{+0.4}_{-0.4}$	$0.2^{+0.2}_{-0.1}$	-	$6.5^{+0.6}_{-0.7}$	$0.25^{+0.11}_{-0.08}$	$49.5^{+4.2}_{-3.7}$	$1.3^{+0.3}_{-0.2}$
F06021-4509	C2	$25.8^{+8.9}_{-8.8}$	$0.4^{+0.4}_{-0.3}$	$-1.1^{+0.2}_{-0.2}$	$0.4^{+0.3}_{-0.1}$	$5.0^{+1.2}_{-1.0}$	$0.4^{+0.3}_{-0.3}$	$-1.3^{+0.1}_{-0.1}$	$4.4^{+0.9}_{-0.7}$	$0.09^{+0.01}_{-0.01}$	$59.8^{+1.6}_{-1.8}$	$1.1^{+0.2}_{-0.1}$
F06035-7102	C2 1SAN	$23.2^{+3.6}_{-2.7}$	$0.3^{+0.4}_{-0.2}$	$-1.2^{+0.0}_{-0.0}$	-	$349.8^{+42.2}_{-38.6}$	$0.3^{+0.4}_{-0.3}$	-	$0.4^{+0.0}_{-0.0}$	$0.65^{+0.12}_{-0.11}$	$49.3^{+2.1}_{-1.7}$	$1.1^{+0.1}_{-0.0}$
F06206-6315	C2 1SA	$49.0^{+7.4}_{-8.4}$	$0.6^{+0.6}_{-0.4}$	$-1.3^{+0.2}_{-0.1}$	$0.5^{+0.1}_{-0.1}$	$12.8^{+0.9}_{-1.1}$	$0.5^{+0.4}_{-0.4}$	-	$4.5^{+0.4}_{-0.4}$	$0.67^{+0.13}_{-0.10}$	$45.9^{+1.8}_{-1.8}$	$1.1^{+0.1}_{-0.1}$
F18582-5558	C2	$213.2^{+191.4}_{-85.6}$	$0.3^{+0.4}_{-0.2}$	$-0.9^{+0.1}_{-0.1}$	$0.0^{+0.0}_{-0.0}$	$5.9^{+1.0}_{-0.9}$	$0.1^{+0.1}_{-0.1}$	$-1.3^{+0.2}_{-0.1}$	$5.4^{+0.7}_{-0.9}$	$0.48^{+0.07}_{-0.08}$	$43.4^{+1.5}_{-1.4}$	$1.8^{+0.1}_{-0.2}$
F20117-3249	C2 1SAN	$7.3^{+1.7}_{-1.3}$	$0.6^{+0.6}_{-0.4}$	$-1.1^{+0.1}_{-0.1}$	-	$73.0^{+3.4}_{-2.9}$	$0.5^{+0.6}_{-0.4}$	-	$1.6^{+0.2}_{-0.2}$	$1.14^{+0.57}_{-0.38}$	$37.1^{+2.5}_{-2.1}$	$1.7^{+0.2}_{-0.3}$
F20445-6218	C	$62.0^{+106.3}_{-15.7}$	$0.6^{+0.5}_{-0.4}$	$-0.8^{+0.1}_{-0.1}$	$0.2^{+0.1}_{-0.2}$	-	-	-	-	$0.40^{+0.24}_{-0.10}$	$46.6^{+3.1}_{-3.9}$	$1.3^{+0.3}_{-0.2}$
F21178-6349	C	$28.6^{+9.1}_{-7.0}$	$0.9^{+0.2}_{-0.2}$	$-1.2^{+0.1}_{-0.1}$	$0.4^{+0.1}_{-0.1}$	-	-	-	-	$0.23^{+0.15}_{-0.08}$	$48.2^{+4.6}_{-4.4}$	$1.5^{+0.4}_{-0.3}$
F21292-4953	PL	$21.0^{+0.6}_{-0.7}$	-	$-0.5^{+0.0}_{-0.0}$	-	-	-	-	-	$0.46^{+0.25}_{-0.13}$	$46.7^{+3.5}_{-3.6}$	$1.4^{+0.4}_{-0.3}$
F21295-4634	C2 1SAN	$1.1^{+0.7}_{-0.6}$	$0.3^{+0.2}_{-0.2}$	$-1.0^{+0.1}_{-0.1}$	-	$31.3^{+7.7}_{-6.1}$	$0.3^{+0.3}_{-0.2}$	-	$0.5^{+0.2}_{-0.1}$	$1.27^{+0.54}_{-0.44}$	$39.0^{+2.9}_{-2.2}$	$1.6^{+0.2}_{-0.3}$
F23389-6139	C2 1SA	$421.7^{+14.4}_{-14.6}$	$1.0^{+0.6}_{-0.7}$	$-1.4^{+0.0}_{-0.0}$	$0.4^{+0.0}_{-0.0}$	$91.9^{+6.8}_{-6.5}$	$0.7^{+0.6}_{-0.4}$	-	$3.0^{+0.2}_{-0.2}$	$0.86^{+0.26}_{-0.23}$	$44.7^{+2.7}_{-2.3}$	$1.3^{+0.3}_{-0.2}$

T. Galvin, Seymour, et al. (submitted)

Thermal Fractions

Lower thermal fraction than for M82 (~10%)

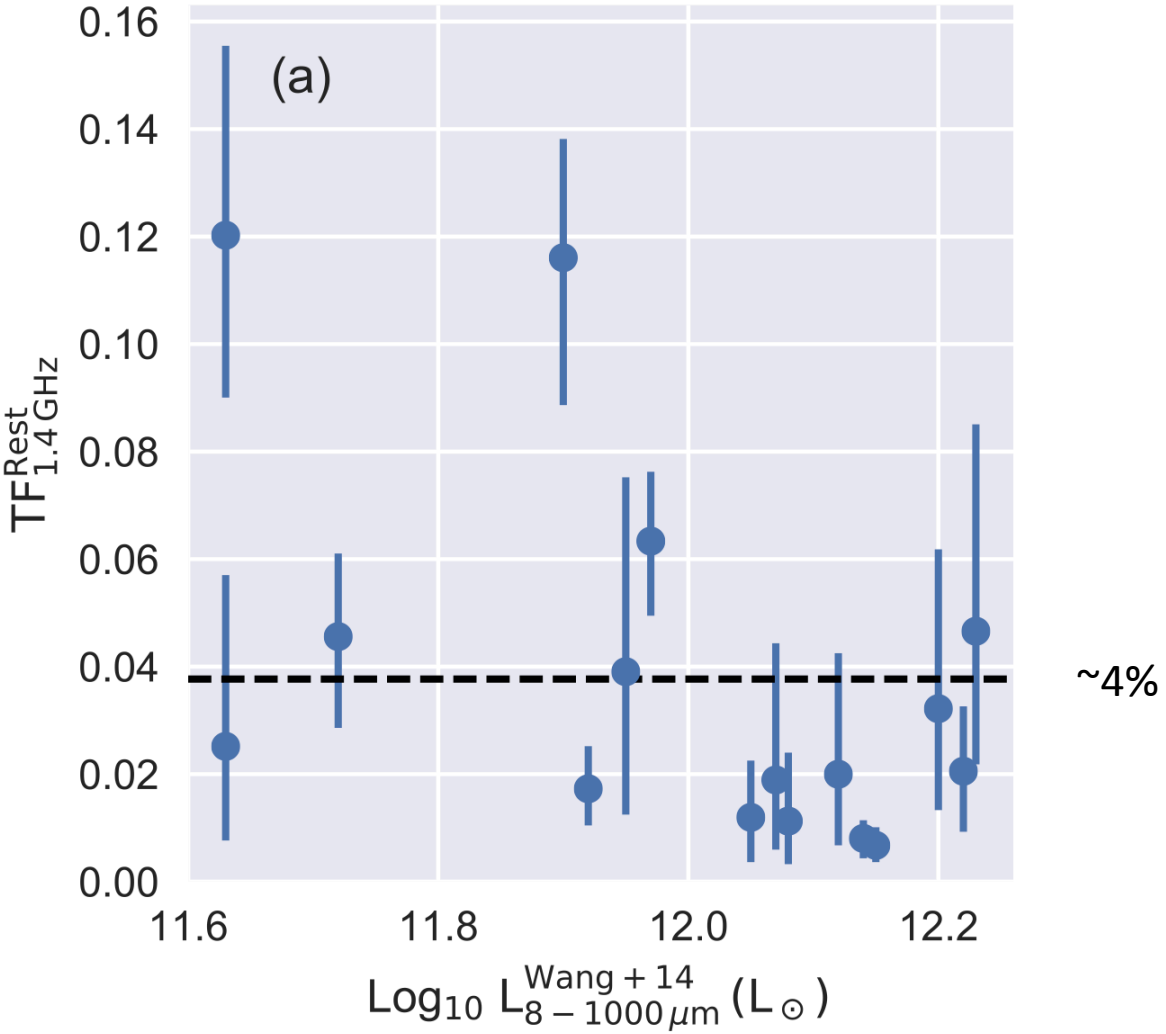

T. Galvin, Seymour, et al. (submitted)

Spectral Index

$\langle \alpha_{syn} \rangle \sim -0.98$

$\alpha = -1.0$

Is intrinsic synchrotron steeper than $\alpha = -0.7$?

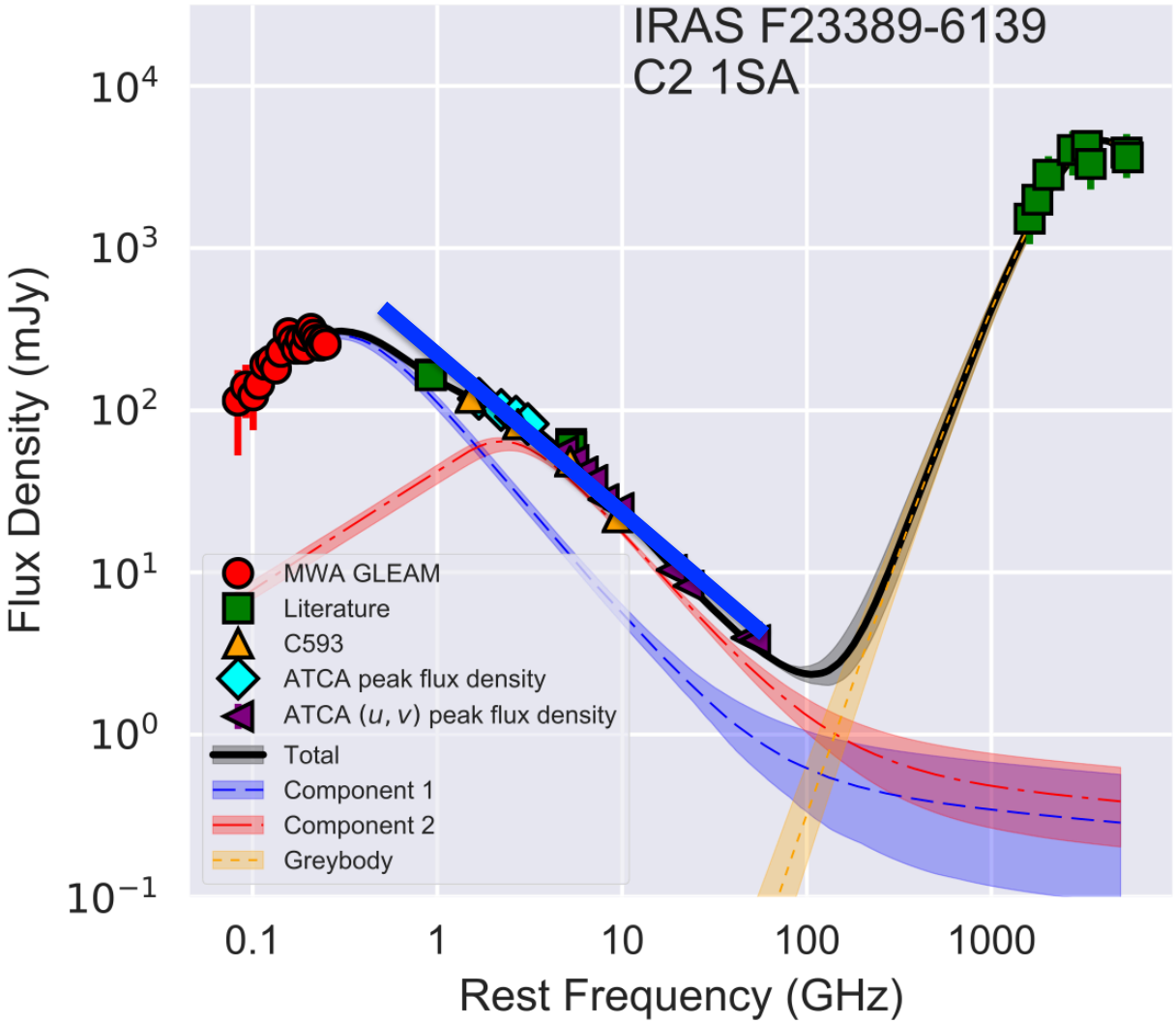

T. Galvin, Seymour, et al. (submitted)

Spectral Index

$\langle \alpha_{syn} \rangle \sim -0.98$

$\alpha = -1.0$

$\alpha = -0.7$

Is intrinsic synchrotron steeper than $\alpha = -0.7$?

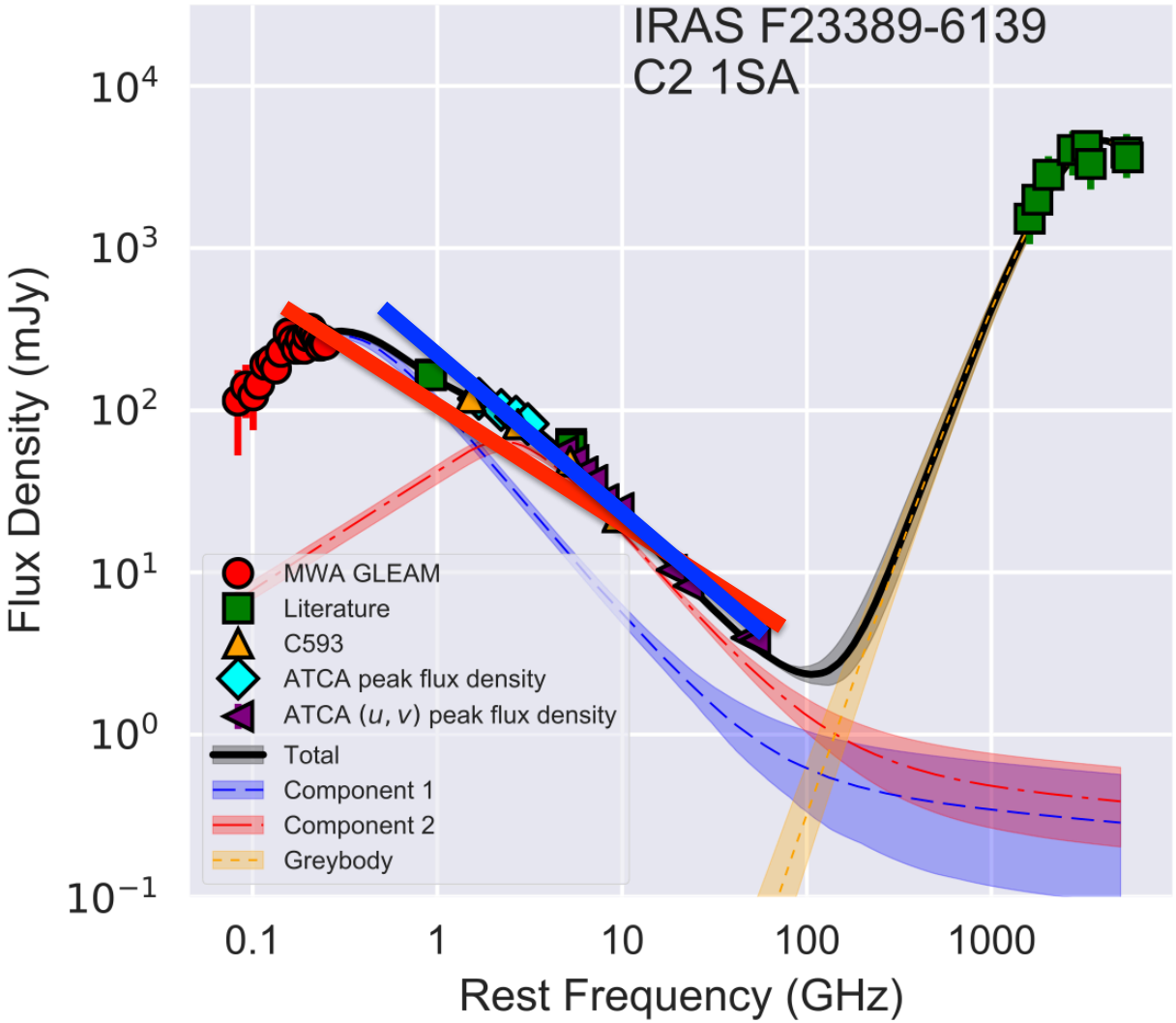

T. Galvin, Seymour, et al. (submitted)

Spectral index v SFR

Radio spectral index from cosmic ray index estimated from GeV to TeV observations (Wang & Fields, 2017)

Do higher SFR galaxies have steeper cosmic ray (and therefore synchrotron) spectral index?

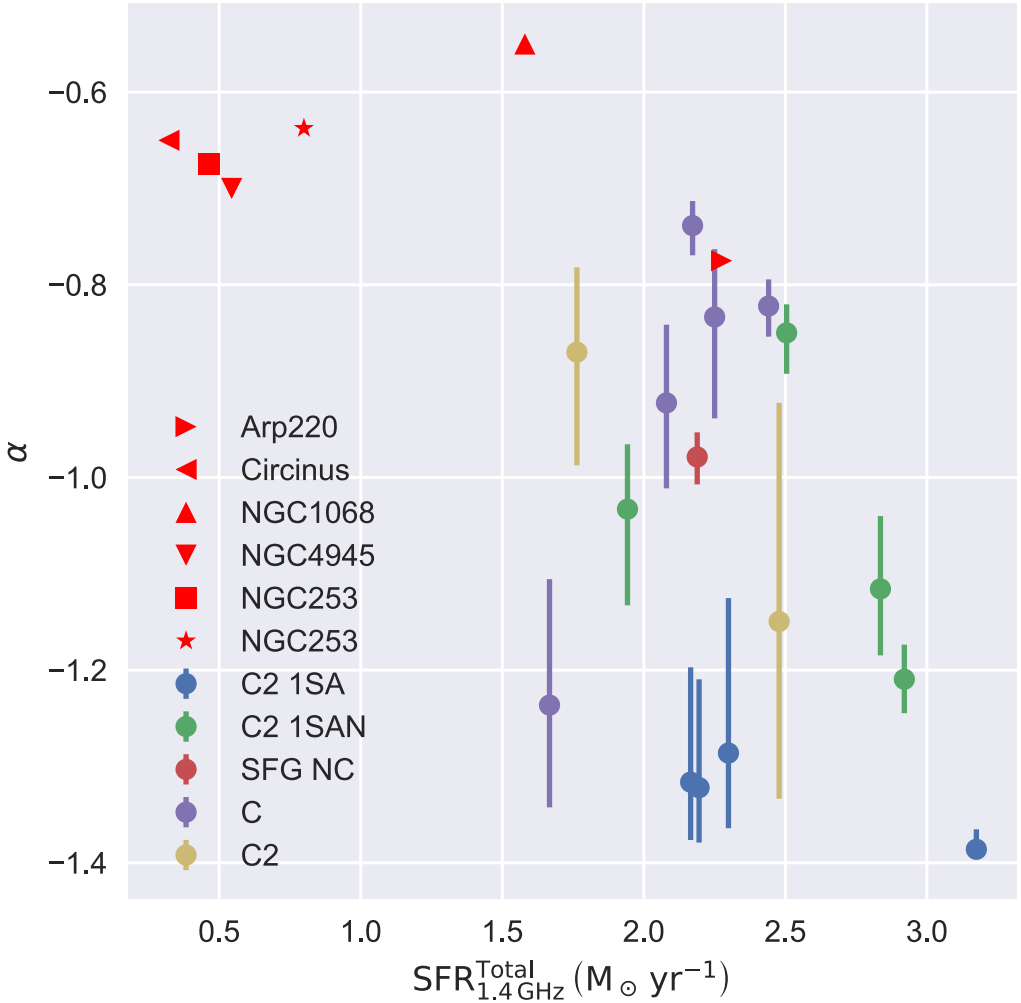

Emission Measures

Source *IRAS*	EM_1 $10^6\,\mathrm{cm}^{-6}\,\mathrm{pc}$	EM_2 $10^6\,\mathrm{cm}^{-6}\,\mathrm{pc}$
F00198-7926	0.016	13.836
F00199-7426	0.021	–
F01388-4618	0.02	–
F02364-4751	0.017	–
F03068-5346	0.005	–
F04063-3236	0.029	15.933
F06021-4509	0.038	6.197
F06035-7102	–	0.044
F06206-6315	0.057	6.471
F18582-5558	0.014	8.074
F20117-3249	–	1.002
F20445-6218	0.023	–
F21178-6349	0.042	–
F21295-4634	–	0.079
F23389-6139	0.04	3.099

$$\tau_\nu = 3.28 \times 10^{-7} \left(\frac{T_e}{10^4\,\mathrm{K}}\right) \left(\frac{\nu}{\mathrm{GHz}}\right)^{-2.1} \left(\frac{EM}{\mathrm{pc\,cm}^{-6}}\right)$$

$$\frac{EM}{\mathrm{pc\,cm}^{-6}} = \int_{\mathrm{los}} \left(\frac{N_e}{\mathrm{cm}^{-3}}\right)^2 d\left(\frac{s}{\mathrm{pc}}\right)$$

T. Galvin, Seymour, et al. (submitted)

Optical Geometry

WiFeS IFU Observations

Star Formation Rate

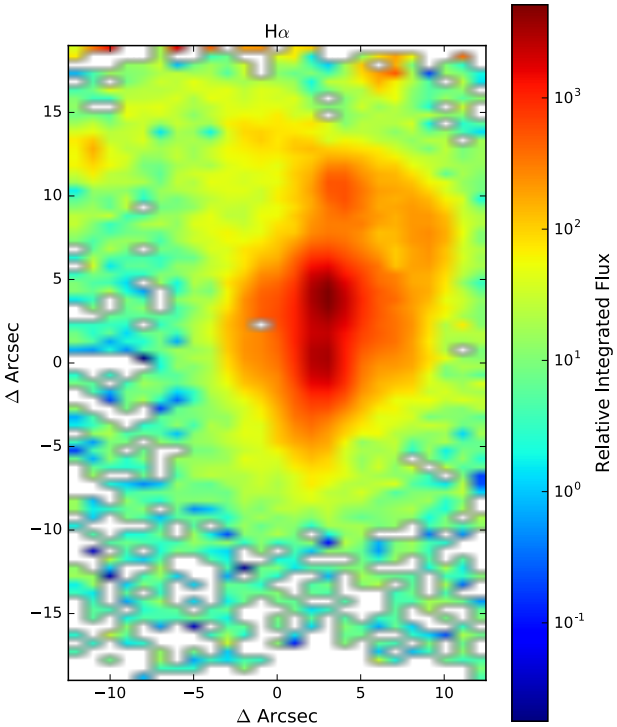

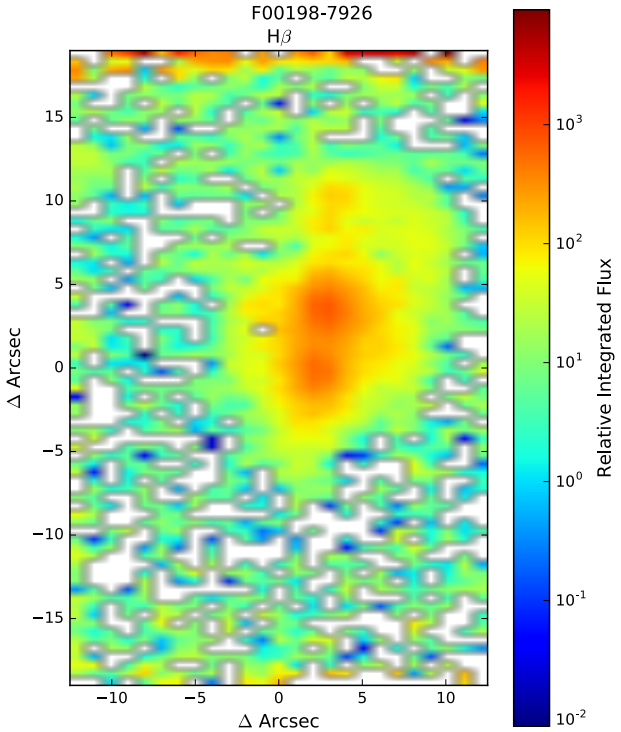

Dust distribution

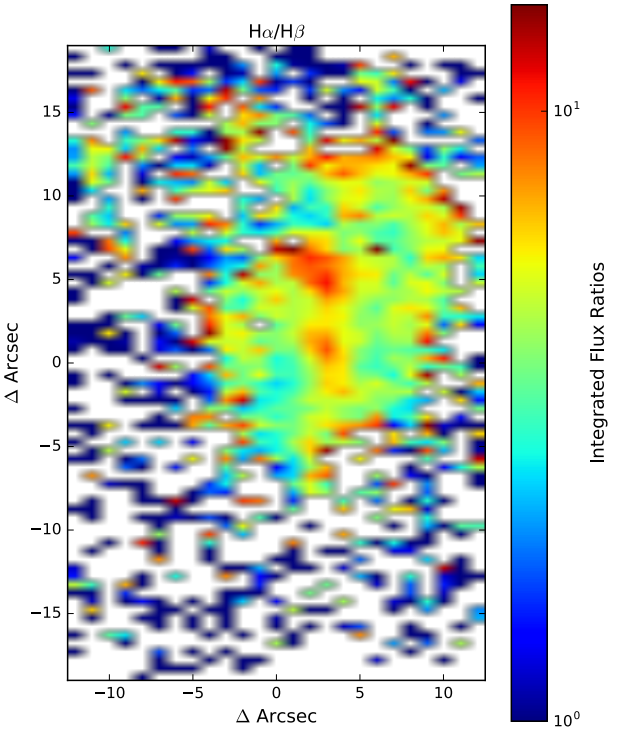

Galvin, Seymour, et al. (in prep.)

Suppression of Low Frequency Flux

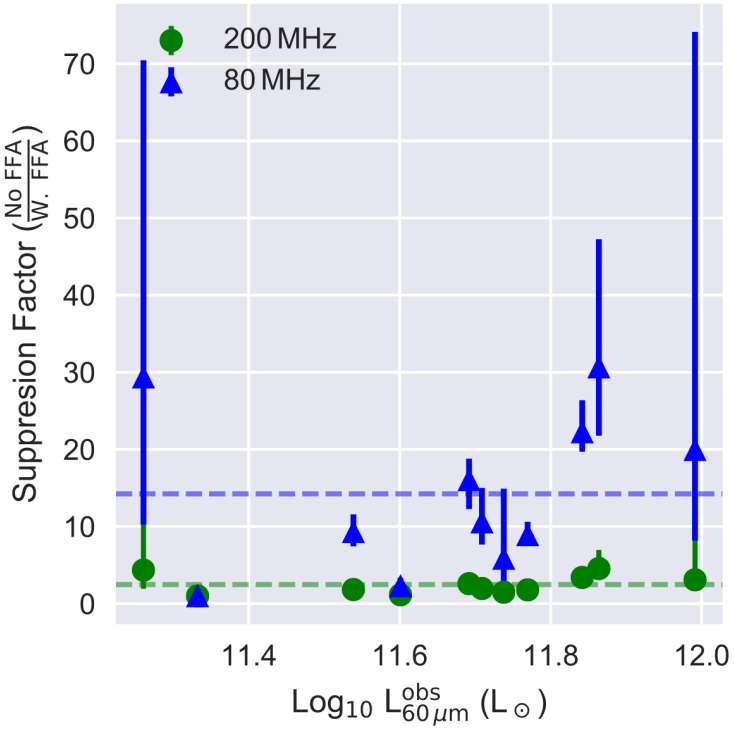

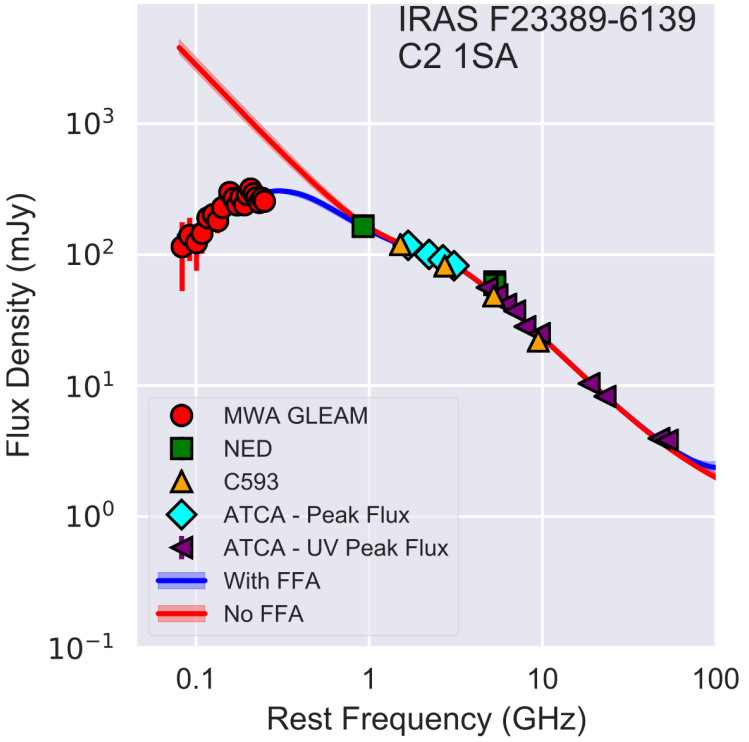

Conclusions

- The radio SEDs of SFGs are surprisingly complex revealing often revealing multiple components with low-frequency turn-overs which is most likely due to geometry of star formation
- Lower thermal fraction than lower SFR galaxies
- Evidence that the intrinsic synchrotron spectral indexes are steeper than -0.7
- Implications for deep source counts

ICRAR

International Centre for Radio Astronomy Research

We acknowledge the Wajarri Yamatji people as the traditional owners of the observatory site.

Curtin University

The Government of Western Australia

The University of Western Australia